Physiological and Microfluorometric Studies of Reduction and Clearance of Retinal in Bleached Rod Photoreceptors

Efthymia Tsina,[1] Chunhe Chen,[2] Yiannis Koutalos,[2] Petri Ala-Laurila,[1]
Marco Tsacopoulos,[3] Barbara Wiggert,[4] Rosalie K. Crouch,[5] and M. Carter Cornwall[1]

[1]Department of Physiology and Biophysics, Boston University School of Medicine, Boston, MA 02118
[2]Department of Physiology and Biophysics, University of Colorado School of Medicine, Denver, CO 80262
[3]Department of Experimental Physiology, University of Athens, Athens, Greece
[4]National Eye Institute, National Institutes of Health, Bethesda, MD 20892
[5]Department of Ophthalmology, Medical University of South Carolina, Charleston, SC 29425

ABSTRACT   The visual cycle comprises a sequence of reactions that regenerate the visual pigment in photoreceptors during dark adaptation, starting with the reduction of all-trans retinal to all-trans retinol and its clearance from photoreceptors. We have followed the reduction of retinal and clearance of retinol within bleached outer segments of red rods isolated from salamander retina by measuring its intrinsic fluorescence. Following exposure to a bright light (bleach), increasing fluorescence intensity was observed to propagate along the outer segments in a direction from the proximal region adjacent to the inner segment toward the distal tip. Peak retinol fluorescence was achieved after ∼30 min, after which it declined very slowly. Clearance of retinol fluorescence is considerably accelerated by the presence of the exogenous lipophilic substances IRBP (interphotoreceptor retinoid binding protein) and serum albumin. We have used simultaneous fluorometric and electrophysiological measurements to compare the rate of reduction of all-trans retinal to all-trans retinol to the rate of recovery of flash response amplitude in these cells in the presence and absence of IRBP. We find that flash response recovery in rods is modestly accelerated in the presence of extracellular IRBP. These results suggest such substances may participate in the clearance of retinoids from rod photoreceptors, and that this clearance, at least in rods, may facilitate dark adaptation by accelerating the clearance of photoproducts of bleaching.

KEY WORDS: retinol • vitamin A • photoreceptor • visual cycle • IRBP

INTRODUCTION

The absorption of a photon by the visual pigments in the outer segment of vertebrate rod photoreceptors is the initial event in the activation of the visual phototransduction cascade. This event triggers a rapid photoisomerization of the chromophore retinal embedded within the pigment from the 11-cis to the all-trans conformation to form metarhodopsin II (Meta II), the activated form of the pigment. Meta II then catalyzes the exchange of GTP for GDP on the α-subunit of the G-protein transducin and initiates a cascade of reactions, which results in enzymatic destruction of cGMP, a closure of cation channels in the plasma membrane, and a decrease of transmitter release by photoreceptor synaptic processes onto secondary retinal neurons (for review see Pugh and Lamb, 2000).

For the rod photoreceptor to recover fully from previous light exposure, photoactivated (bleached) pigment must be regenerated to a form containing 11-cis retinal. In the vertebrate retina, pigment regeneration is a complex process, referred to as the visual cycle, requiring the participation of both the photoreceptors and the retinal pigment epithelium (RPE), a layer of tissue lying immediately behind and adjacent to the retina. Regeneration can be thought to begin with the reduction of all-trans retinal to all-trans retinol within photoreceptor outer segments. All-trans retinol is then transported from the outer segments and is taken up by substances in the interphotoreceptor matrix, a complex of substances located in the extracellular space surrounding the photoreceptors. The most important of these is likely to be interphotoreceptor retinoid-binding protein (IRBP) (Adler et al., 1985; Redmond et al., 1985), but other fatty acid binding proteins may be involved as well (Adler and Edwards, 2000). The retinol is then translocated to the RPE (Okajima et al., 1990), where it is stored in a detoxified form as a retinyl ester (Saari et al., 1993) and isomerized to the 11-cis form (Bernstein and Rando, 1986; McBee et al., 2000)

by a complex process that is still poorly understood (McBee et al., 2000). Finally, 11-cis retinol is oxidized to 11-cis retinal and transported back to the receptor outer segments where it conjugates with opsin to form visual pigment.

Though the reduction of retinal to retinol was the first reaction of the visual cycle to be identified (Wald and Hubbard, 1949), little was known about the structure and function of the all-trans retinol dehydrogenase (RDH) until recently. This enzyme is a 34-kD protein that is tightly associated with outer segment membranes (Palczewski et al., 1994; Rattner et al., 2000). RDH uses nicotine adenine dinucleotide phosphate (NADPH) as a cofactor (Futterman et al., 1970; Palczewski et al., 1994) rather than NADH as first supposed (Wald and Hubbard, 1949). It shows a substantial preference for all-trans retinal over 11-cis retinal (Lion et al., 1975; Palczewski et al., 1994). Exactly how this reduction takes place, and how it is related to quenching of the visual transduction cascade and subsequent retinol transport, is still a matter of controversy. Additionally, it is not known if reactions that fuel the reduction are located exclusively in the outer segment, or whether reducing equivalents are generated in the energy-rich ellipsoid region located in the inner segment as well. RDH not only plays an important role in quenching of the transduction cascade, but dysfunction of the reduction and transport of retinal from the photoreceptor has been implicated as the proximate cause of Stargardt's disease (Rattner et al., 2000).

The experiments described here were designed to answer two questions in rod cells isolated from the retina of the tiger salamander. First, we wished to determine the relative contribution of the outer and inner segment of these cells in generating and maintaining levels of NADPH that are necessary for the conversion of retinal to retinol following pigment bleaching. Second, we wished to see if the accelerated clearance of retinoid from bleached photoreceptors by IRBP can facilitate the recovery of flash responsiveness following pigment bleaching. We made use of the observation that all-trans retinol but not all-trans retinal or 11-cis retinal can be excited by near UV light to emit bright green fluorescent light (Kuhne, 1879; Kaplan, 1985). We used this intrinsic fluorescence to monitor the spatial distribution and time course of retinol formation and its clearance within the outer segments of salamander rods before and following intense bleaching light. Our results demonstrate that retinal is reduced to retinol over the course of tens of minutes in rods. This reaction spreads as a wave along the long axis of the bleached outer segments; reduction occurs first in the area of the outer segment adjacent to the inner segment, and last in the distal tip. Furthermore, transport/clearance of retinol requires factor(s) exclusive of the photoreceptor itself (i.e., located in the interphotoreceptor matrix). Finally, we show that the facilitated clearance of retinoid from these rods by IRBP modestly accelerates the recovery of light responses in darkness after exposure to a bright bleach.

MATERIALS AND METHODS

All experiments were performed according to procedures approved by the Animal Use and Care Committees of Boston University School of Medicine and University of Colorado Health Sciences Center as being consistent with humane treatment of laboratory animals, and with standards set forth in the Guide for the Care and Use of Laboratory Animals and the Animal Welfare Act.

Red rod photoreceptors were mechanically isolated from dark-adapted retinae of larval and adult tiger salamander (*Ambystoma tigrinum*) by methods that have been described previously (Cornwall et al., 1990). A small portion of the resulting suspension was placed in a chamber located on the stage of an inverted microscope (Nikon Eclipse TE300; Nikon), where individual cells were viewed using an infrared television camera and monitor fitted to the microscope.

Fluorescence Measurements

The experimental setup is illustrated in Fig. 1. The inverted microscope was configured for use in conventional epifluorescence mode. An intense beam of light from a xenon continuous arc (Optosource Arc Lamp and power supply; Cairn Instruments) was passed through neutral density filters, a 360-nm narrow-band interference filter (Chroma Technology), and electronic shutter (Vincent Associates) before entering the microscope fluorescence port. The focused beam of light was then reflected upward by a dichroic mirror (400DCLP; Chroma Technology), and focused by a microscope objective (Nikon 100× S Fluor; Nikon) on to the photoreceptor cells located in the chamber on the stage of the microscope. An example of a bright-field image of two rod cells is shown at the top of Fig. 1. Different regions of the cell shown to the right of the field have been outlined in red. These regions (from top to bottom) are as follows: four regions of the outer segment containing the visual pigment, the ellipsoid region of the cell body that contains mitochondria, and the remainder of the cell body containing the nucleus. The four outer segment regions between the distal tip of the outer segment and the ellipsoid are referred to as the distal, mid-distal, mid-proximal, and proximal in subsequent analyses. The synaptic endings normally attached to the cell body were normally removed when cells were dissociated from the whole retina. Fluorescent light emitted from the photoreceptors, resulting from exposure to a 200-ms step of 360-nm excitation light, was collected by the microscope objective, passed through the dichroic mirror, and a wide-band emission filter (D510/80M; Chroma Technology) that transmits between 465 and 550 nm, and then focused on the face of an image intensifier (VS4-jonesal CCD camera [Cool Snap FX; Roper Scientific Inc.]). The spatial distribution of fluorescence before and at various times following exposure to a bright 520-nm light calculated to have bleached >99% of the visual pigment, was detected by the camera. The output of the camera was converted to a pseudocolor image, as illustrated at the bottom of Fig. 1. Areas of least fluorescence are illustrated in blue; intermediate levels by green and yellow, and the most intense levels by red. Regional differences in fluorescence as outlined by the areas shown in red in the bright field image were measured at different times before and after exposure of the cells to bleaching light.
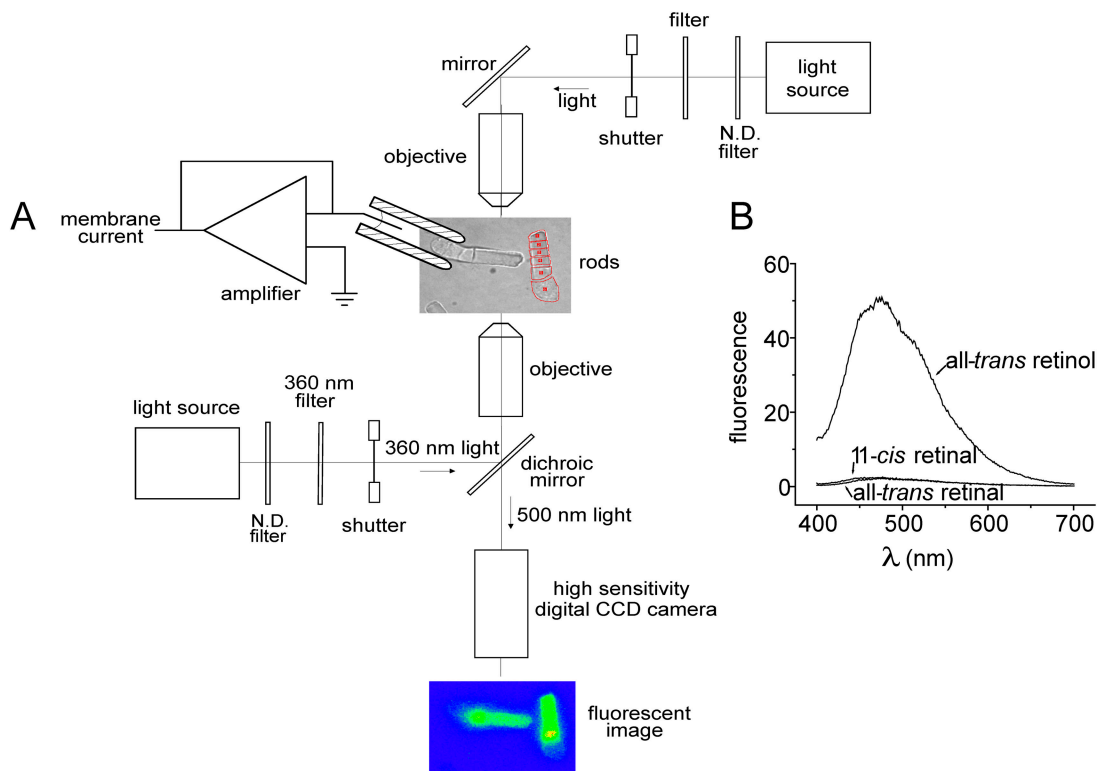
FIGURE 1. Schematic representation of the experimental apparatus. The arrangement of the inverted microscope and fluorescence excitation light source is shown at left. (A) Bright-field image of two rod photoreceptors is shown at the top and a pseudocolor fluorescent image of these cells is shown at the bottom. A recording electrode holding the inner segment of the left cell shown in the bright-field image is connected to a recording amplifier. The light source at the top was used for light stimulation during electrophysiological recording as well as bleaching of photoreceptors. The lower light source provided UV fluorescence probe flashes. (B) Plot of fluorescence emission spectra of equimolar (50 μM) ethanolic solutions of 11-cis retinal, all-trans retinal, and all-trans retinol. Fluorescence intensity of all-trans retinol is >50-fold greater than that of 11-cis retinal or all-trans retinal.

The principal fluorophore in which we were interested was all-trans retinol, which appears in the outer segment, reduced from all-trans retinal after bleaching. The fluorescence excitation spectrum of all-trans retinol extends from ~250 nm to 350 nm. As shown in Fig. 1 B, the emission spectrum is very broad, extending over 100 nm on either side of its peak. Also shown are the emission spectra of all-trans and 11-cis retinal. Comparison of these fluorescence emission spectra shows that the fluorescence intensity of all-trans retinol in ethanol is more than 50-fold greater than equimolar solutions of either all-trans or 11-cis retinal.

Although larval tiger salamander rods contain a mixture of A_1 and A_2 retinal pigments, the observed fluorescence signal from the outer segments is dominated by A_1 all-trans retinol, as its quantum yield is 37-fold higher than that of A_2 (Tsin et al., 1988), and A_1 comprises only 20–30% of the total chromophore (Cornwall et al., 1984). In some experiments, the A_1/A_2 pigment concentration ratio within single isolated photoreceptor outer segments was estimated by fitting a linear combination of A_1 and A_2 pigment absorption templates to individual visual pigment absorbance spectra obtained using a photon-counting microspectrophotometer (Cornwall et al., 1984; Govardovskii et al., 2000). The acquisition and subsequent processing of fluorescence images employed a conventional microcomputer and imaging software (Open lab; Improvision).

For comparisons of total outer segment fluorescence across different cells, fluorescence intensities were normalized to the maximal steady-state value, obtained by fitting the fluorescence rise with a single exponential. For comparisons of fluorescence across different outer segment areas, fluorescence intensities were normalized to the maximal retinol fluorescence of the proximal part as follows: the basal, nonretinol fluorescence (obtained from the first, prebleach image) was subtracted from all fluorescence intensities; the intensities were then divided by the maximal, steady-state value of the retinol fluorescence in the proximal part, obtained by fitting the fluorescence rise with a single exponential.

Experiments with exogenous retinoids were performed in a manner similar to that described above, but using instead an inverted Zeiss Axiovert 100 microscope (Carl Zeiss MicroImaging, Inc.), a xenon continuous arc light source from Sutter Instrument Company, a Zeiss 40× Plan Neofluar objective lens, a Sensi-Cam CCD camera (Cooke Corporation), and Intelligent Imaging Innovations software.

Electrophysiological Recording

Measurements of membrane current were made extracellularly, as illustrated in Fig. 1 A, by methods that have been described previously (Baylor et al., 1979; Cornwall et al., 1990; Corson et al., 2000). The current recorded from the cell was converted to voltage, amplified, and low-pass filtered with an active eight-pole filter at 20 Hz cut-off frequency. Data were digitized at 250 Hz, stored on a computer, and subsequently analyzed using pCLAMP

431   TSINA ET AL.

8 data acquisition and analysis software (Axon Instruments, Inc.) and the Origin 4 graphics analysis software (Microcal Software).

Solutions

The chamber in which fluorescence measurements were made was superfused with a saline solution that contained (in mM) 110 NaCl, 2.5 KCl, 1.6 MgCl$_2$, 1.0 CaCl$_2$, 10 dextrose, 10 HEPES, pH 7.8. BSA (100 mg/liter) was present except where indicated. Entry of solution into the chamber was via a gravity-fed inlet supplied by a reservoir; outlet was via a tissue wick located in a trough positioned at one end of the chamber. Test solutions were added to the bath by an inlet line from an additional reservoir or by direct addition using a standard laboratory pipetter. Before each experiment, the chamber was treated with a 1% aqueous solution of concanavalin A in 2 M NaCl (Type IV; Sigma-Aldrich) to promote adherence of the cells to the bottom of the chamber. If addition of test solutions to the experimental chamber during a series of fluorescence measurements caused the cells to change their position within the chamber, the experiment was terminated.

Photostimulation and Pigment Bleaching

The optical stimulator providing the bleaching light is illustrated at the top of Fig. 1. It consisted of a shuttered light source with neutral density and interference filters to define the wavelength, intensity, and duration of bleaching light. A mirror and a 10× microscope objective mounted in the condenser assembly of the microscope directed this light to a 400-μm spot of uniform intensity located at the plane of the preparation. The intensity of this spot (I_B) was calibrated at the beginning of each experiment with a photometer (model 80X; United Detector Technology) to an unattenuated intensity of 7.4×10^7 photons micrometer^{-2} s^{-1}.

An estimate of the fractional bleaching of visual pigment by the light stimulator was made on the assumption that the rate of bleaching is proportional to the concentration of pigment times the product of the light intensity, I_B, and the photosensitivity, P, of the visual pigment (Dartnall, 1972). The photosensitivity used for salamander rod photoreceptors containing primarily Vitamin A$_2$ was calculated previously as the product of the absorption cross section and the quantum efficiency for bleaching to be 6.0×10^{-9} μm^2 (Cornwall et al., 2000). The fraction of pigment, F, that is bleached after a light step of duration t and intensity I_B was calculated from the following relationship: $F = \{1 - \exp(-I_B Pt)\}$.

RESULTS

Fig. 2 displays images and graphical representations of the spatial distribution of fluorescence in isolated rods before and at different times after exposure to a bright bleaching light. Fig. 2 A (left) shows a bright-field image as well as three pseudocolor fluorescence images of the two rods illustrated in Fig. 1. The images were taken 1 min before (top right) and 5 min (bottom left) and 31 min (bottom right) after exposure to a light calculated to have bleached >99% of the pigment. Prior to bleaching, a persistent spatially localized fluorescence was observed to be restricted to the ellipsoid region of the cell; little fluorescence was observed in the outer segments or other regions of the cells. The fluorescence in the ellipsoid regions was relatively stable, generally increasing only slightly after the bleach. After
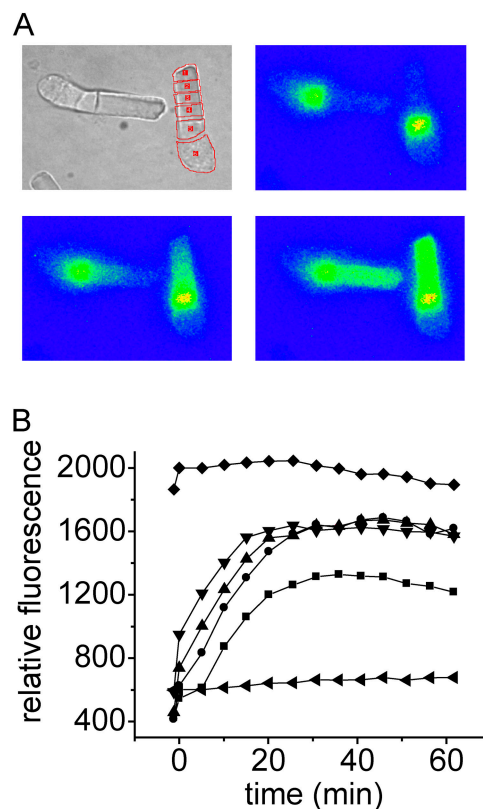

FIGURE 2. Fluorescence images of rod photoreceptor cells before and following photopigment bleaching. (A) Bright-field image of two salamander rods (upper left) together with three fluorescent images taken before (upper right) and 5 min (bottom left) and 31 min (bottom right) after bleaching. (B) Time course of fluorescence changes resulting from bleaching of the cell shown in A (right). Integrated fluorescence measurements were made in the cell body (◀), ellipsoid (◆), proximal outer segment (▼), mid-proximal outer segment (▲), mid-distal outer segment (●), and distal tip of the outer segment (■). These areas are outlined in red in bright-field image. Time = 0 on the abscissa corresponds to the end of 10 s bleaching light.

bleaching, however, a large and persistent spatially localized fluorescence was observed to increase in the outer segments over the subsequent 30–45 min. A fluorescence increase similar to this has been observed in bleached frog rods where it has been attributed to all-trans retinol (Liebman, 1969, 1973; Kaplan, 1985), produced by the reduction of all-trans retinal by RDH and NADPH (Futterman et al., 1970).

After a bleach of uniform light intensity across the whole cell, increasing fluorescence intensity was observed to propagate along the outer segments in a direction from the proximal region adjacent to the cell body/ellipsoid region of the cell toward the distal tip of the outer segment. Fig. 2 B shows a plot of the fluorescence signal from the cell shown on the right in the bright-field image of Fig. 2 A, measured in the different regions outlined in red at different times after the uniform bleach. It can be seen from this plot that an in-

creased level of fluorescence appeared within about a minute after the bleach in the region adjacent to the ellipsoid (Fig. 2 B, inverted triangles) and spread in the direction toward the distal tip of the outer segment. Fluorescence intensity in the intermediate regions (Fig. 2 B, upright triangles, filled circles) increased more slowly. Fluorescence in the distal tip (Fig. 2 B, filled squares) increased most slowly and by a lower total amount.

Fig. 3 plots average fluorescence data of the type presented in Fig. 2. Fig. 3 A shows the time course of the average fluorescence changes measured in four outer segment regions in seven different rod outer segments. These data were obtained from cells in which both the inner and outer segments were intact. As was shown in Fig. 2 B, fluorescence was observed on average to increase first in proximal regions of the outer segment, and last in the distal tip of the cell. Fig. 3 B plots the time course of the average fluorescence change, integrated over the entire outer segment, and shows that the increase in fluorescence was complete in ~40 min. The smooth curve in red was fitted to the data assuming a single exponential process with a time constant of 14.3 min.

The data in Figs. 2 and 3 confirmed that the fluorescence increases that occurred in rod outer segments after a uniform bleach spread as a wave, increasing first in the proximal region of the outer segment and later in the distal tip. The integrated fluorescence level in the entire rod outer segments after bleaching reached 90% of its final value in ~34 min after the bleach (Fig. 3 B). Additionally, an initial rapid increase in fluorescence that was between 10 and 20% of maximum fluorescence (Fig. 3, A and B, left side of plot) was observed very soon after bleaching (see DISCUSSION).

Interpretation of these data is complicated by the fact that larval tiger salamander rods contain a mixture of two variants of visual pigment that differ from one another in the structure of their chromophore moieties. The vitamin A_1 rhodopsin is composed of 11-cis retinal covalently attached to opsin, whereas the vitamin A_2 form contains 11-cis 3–4 dehydroretinal as the chromophore moiety. Previous in vitro measurements have demonstrated that the quantum efficiency of fluorescence of vitamin A_1 retinol is 37-fold greater than that of vitamin A_2 retinol (Tsin et al., 1988). This raises the possibility that our measurements are dominated by fluorescence from the vitamin A_1 form of the visual pigment, even though there is less of this form in larval salamander photoreceptors, and that the wave-like appearance of fluorescence after bleaching is an artifact of the mixture of visual pigments variants. To evaluate this complication, we compared post-bleach fluorescence measurements made in rods isolated from larval (aquatic) salamanders that contained an average of
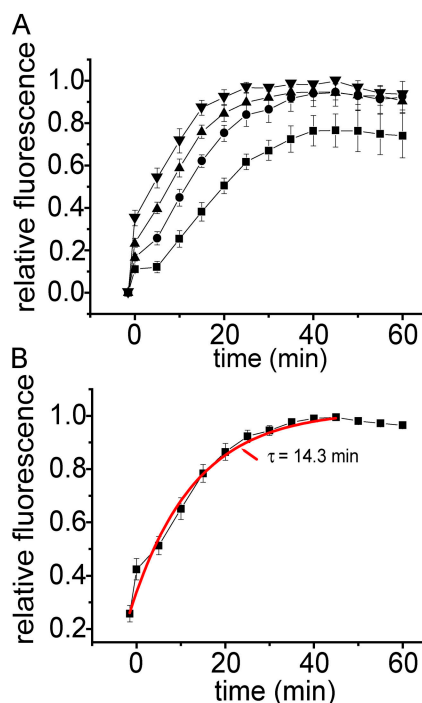

FIGURE 3. Time course of average fluorescence measurements in different outer segment regions of intact isolated rod photoreceptors. (A) Time course of changes in fluorescence (mean ± SEM, $n = 7$) in four different bleached rod outer segment regions: proximal (▼), mid-proximal (▲), mid-distal (●), and distal tip (■). (B) Time course of integrated fluorescence change after bleaching in the entire outer segment. The smooth red curve is an exponential curve fitted to the ensemble of averaged data points (time constant, $\tau = 14.3$ min). Data points in B were not corrected for prebleach fluorescence as in A. Experimental parameters were the same as in Fig. 2.

26.3% vitamin A_1 with measurements made in rods from adult (land phase) salamanders that contained an average of 47.6% vitamin A_1. The measurements of A_1/A_2 pigment fractions were made in these two populations of rod cells by convolving pure A_1 and A_2 pigment spectral templates to individual visual pigment spectra measured microspectrophotometrically. The average increase in fluorescence intensity measured in adult rods compared with larval rods was between two- and threefold. The ratio of the average A_1 pigment concentration in adult salamander rods compared with that in larval salamander rods was measured microspectrophotometrically to be 1.8. Fluorometric and microspectrophotometric measurements were made in rods isolated from the same retina. Thus, the greater amount of A_1 pigment compared with A_2 pigment in adult rod photoreceptors is consistent with the more intense fluorescence that we measured in these cells. Thus, despite the large variations in the A_1/A_2 pigment contcentration ratio in these cell types, the wave-like production of fluorescence in outer segments after bleaching was preserved.

The wave-like increase of fluorescence that occurred in rods after bleaching could be due to spatial differences in the kinetics of the production of all-trans retinol from all-trans retinal, or it could arise from other freely diffusible fluorescent substances such as NADPH or NADH, generated either within the outer segment or in the ellipsoid region of the cell after bleaching. The latter substances might be expected to diffuse to the outer segment of the photoreceptor through the ciliary neck located between the inner and outer segment. They would be expected then to distribute themselves uniformly by diffusion throughout the outer segment within a few tens of seconds (Lamb et al., 1981; Cornwall et al., 1983), and their concentration would be expected to be lowest in the region of the outer segment that was bleached. However, if the fluorescent substance were retinol, it would not be expected to be so freely diffusible, and would be more tightly confined to regions of the cell where photobleaching had occurred, as has been demonstrated previously (Liebman and Entine, 1974; Kaplan, 1985).

To test the importance of the inner segment/ellipsoid region of the cell for this wavelike production of fluorescence, the experiments illustrated in Fig. 4 were performed. Measurements of the level of fluorescence were made in different regions and at different times after a uniform bleach of rod outer segments that had been isolated from the inner segment and ellipsoid regions of the cell. The objective of this experiment was to test the extent to which reducing equivalents important for the reduction of retinal might be supplied from the inner segment or the ellipsoid region of the cell. Fig. 4 A plots average measurements of fluorescence made in four different regions of seven isolated and intact rod outer segments for up to 60 min after a uniform 520-nm bright light. This illumination was calculated to have bleached in excess of 99% of the visual pigment. Though these outer segments were isolated from the cell body, it was still possible to identify the proximal and distal regions of these cell fragments based on morphological criteria. The overlapping standard error bars were excluded from the figure for clarity. It can be seen from these plots that the level of fluorescence throughout the outer segments increased by about threefold during the 60 min after the bleach. However, it is also apparent from this figure that the regional differences in the production of fluorescence seen in intact cells are not observed in isolated outer segments. All regions of the outer segments exhibit increases in fluorescence that are statistically indistinguishable at each time point. Furthermore, the total fluorescence increase observed after 60 min is <25% of that observed after a similar time after bleaching of the same magnitude in the outer segments of intact cells. However, the amplitude and time course of the initial
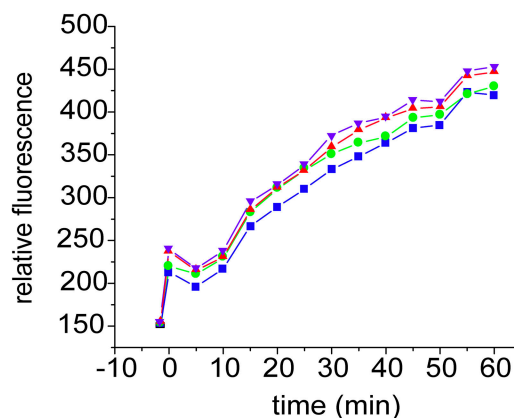

FIGURE 4. Regional changes in outer segment fluorescence. Time course of average fluorescence changes in four regions of seven isolated rod outer segments from which the ellipsoid regions of the cells had been removed. The different regions of the outer segments could be identified by comparison with the geometry of the outer segments of intact cells. Average measurements made from the proximal (▼), the mid proximal (▲), the mid-distal (●), and the distal tip (■) of the outer segments. Symbols and associated connecting lines have been color coded for clarity.

peak of fluorescence observed just after the bleach in these isolated solitary outer segments were similar to those observed in intact cells (Fig. 2 A and Fig. 3 A, compare the early increase in observed fluorescence), suggesting that at this early time, the rates and extents of production of fluorescence were the same whether or not the outer segment was attached to the inner segment. From these experiments, we conclude that reducing equivalents that are supplied from the inner segment are required for the production of the wavelike increase in outer segment fluorescence.

The fluorescence emission spectrum of all-trans retinol significantly overlaps that of reduced NADPH, which is known to be the reducing agent for the conversion of all-trans retinal to all-trans retinol. Furthermore, biochemical mechanisms for the production of NADPH involving glycolysis and the hexose monophosphate pathway have been identified in the rod outer segment (Hsu and Molday, 1994). How can we be sure that the fluorescence we measure is due to retinol and not to a massive light-stimulated production of NADPH that occurs subsequent to light exposure? Previous measurements of the post-bleach fluorescence measured in frog rod outer segments by (Liebman, 1969) have resolved this question. Liebman's work demonstrated that the emission spectrum of this fluorescence (emission peak = 490 nm) is consistent with that of all-trans retinol and not that of NADPH, and that it is polarized parallel to the long axis of the outer segment. Polarization of NADPH fluorescence would not be expected to occur, due to the random orientation of NADPH molecules within the outer segment.
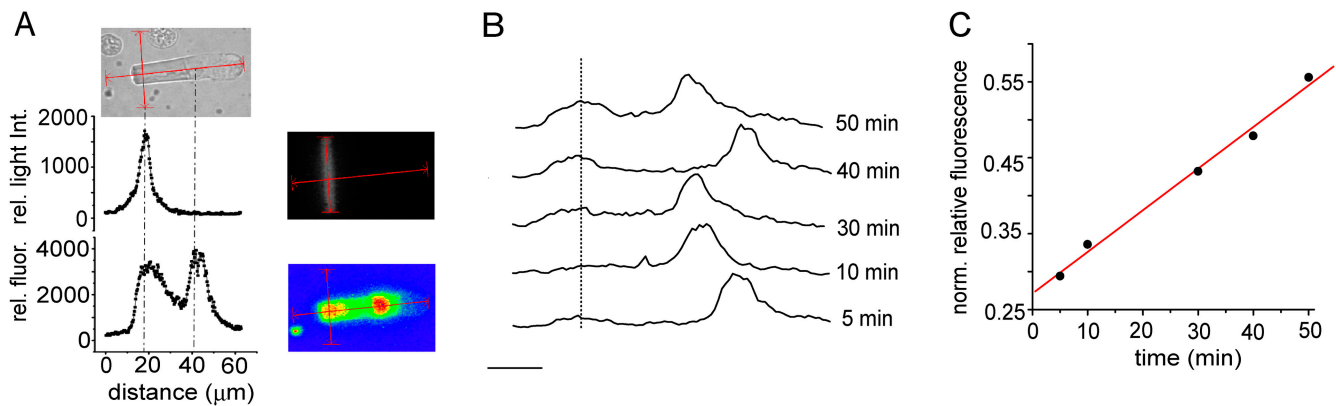
FIGURE 5. Regional fluorescence profiles resulting from a local bleach. (A) Profile of fluorescence changes induced by a focal bleach located at the distal tip of the outer segment of an intact rod. Upper left, bright-field image of a red rod. The vertical red line indicates the locus of a focused slit of intense bleaching light. An image of this slit is shown as the vertical brightness with a red line through its center. Middle left, plot of the relative intensity of this slit as a function of distance along the axial red line. Bottom right, pseudocolor image of the spatial profile of fluorescence measured 60 min after bleach. Bottom left, plot of relative fluorescence intensity along the red line that was projected axially through the cell. Similar results were obtained in 11 other experiments. (B) Fluorescence profiles taken along the long axis of rods at different times after bleaching at the distal tip of the outer segment. The times at which these measurements were made after the bleach are indicated to the right of the traces. The peak fluorescence to the right in each trace is that of the ellipsoid region of the cell; that under the vertical dashed line to the left is the peak fluorescence of the outer segment regions that had been bleached (>99%) at the times indicated. Bar, 10 μm. (C) Plot of the peak fluorescence in the bleached region versus time after the bleach. The red line was fitted to the data by the method of least squares. Fluorescence in the bleached region was calculated as a fraction of the peak fluorescence in the ellipsoid region of the inner segment in each cell. See text for additional experimental details.

The experiments shown in Fig. 5 were performed to measure the extent to which the bleach-induced increase in fluorescence in the outer segment of a rod produced subsequent to exposure to a local slit of intense bleaching light remained spatially restricted for significant periods of time after the bleach. We reasoned that if the bleach-induced fluorescence change were due to the presence of all-trans retinol, it would be expected to be most intense in the light-exposed region of the outer segment, and to be restricted there. On the other hand, if the fluorescence were due to NADPH, it would be expected to be distributed uniformly throughout the outer segment within a short time after the local bleach. The panel shown at the top left of Fig. 5 A is a bright-field image of a solitary isolated intact rod in which the vertical red line indicates the position of a spatially restricted slit of bleaching light. At the beginning of the experiment, this slit was placed at the distal tip of the photoreceptor, using infrared light to which the cell was not responsive. A monochrome image of this slit, taken with the high-sensitivity camera, is shown in the middle right panel in this figure; the graph at the middle left shows a plot of the relative intensity of this slit as a function of distance along the long axis of the cell, where the maximum intensity of the slit illumination is indicated by the position of the vertical red line, located ~5 μm from the distal tip of the cell. This region of the cell was then exposed to a bright light calculated to have bleached >99% of the pigment located under the red line. The

cell was then left for 60 min in darkness, after which the spatial distribution of fluorescence was measured (Fig. 5 A, bottom right panel).

The graph at the bottom left of Fig. 5 A shows the distribution of fluorescence intensity along the longitudinal axis of the cell. From this plot, it is evident that there are two peaks of fluorescence intensity: one located in the ellipsoid region of the inner segment and a second localized in the outer segment region that had been exposed previously to bleaching light. The fluorescence in the ellipsoid region, as illustrated also in Fig. 2, changed little before and after bleaching, and is most likely due to substances such as NADH and NADPH, known to be present in this energy-rich ellipsoid region of the cell that contains mitochondria. The local high level of fluorescence located in the distal part of the outer segment after bleaching, though distributed somewhat more widely than that of the bleaching slit (compare the graphs in Fig. 5 A, middle left and bottom left), appears to be highly restricted to the bleached region.

Figs. 5 (B and C) illustrates the time course of the local increase in outer segment fluorescence that is illustrated in Fig. 5 A. Fig. 5 B presents a series of records of the fluorescence profile measured along the length of rods that had been bleached locally as shown in Fig. 5 A, but measured at different times between 5 and 50 min after exposure to the bleaching slit. Each of these records was made from a single cell. Only one such measurement could be made in each cell because the

test flash that was used to measure the local bleach-induced change in fluorescence also produced an additional uniform bleach of all other regions of the outer segment. The peak fluorescence indicated on the right side of each trace is that measured in the ellipsoid region of the inner segment. The relative magnitude of fluorescence in this region of each cell remained essentially constant. The vertical dashed line to the left in each trace indicates the location of the peak fluorescence intensity in the region of the outer segment that had been bleached locally. Note that the distance between the bleached region and the ellipsoid region was somewhat different in each cell measured, due to the different lengths of the cells studied. The peak light-induced fluorescence change in the locally bleached region of the outer segment was calculated as a fraction of the maximum fluorescence measured in the ellipsoid regions of each of the cells. This is plotted versus time, as shown in Fig. 5 C. The red line that was fitted to these points shows that the rate of increase in locally bleached regions was somewhat less than the integrated outer segment fluorescence observed in the outer segment of rods to which inner segments were attached (see Figs. 2 and 3), but was similar to that observed in truncated outer segments (Fig. 4).

Each of the rods that had been exposed to slit bleaching illumination was subsequently exposed to a uniform bleaching light that was calculated to produce a full bleach of all remaining pigment in the outer segment. The time course of the increase of fluorescence in these initially unbleached regions was then followed for the next 60 min (unpublished data). We observed that the initial rate of increase of fluorescence in the regions of the outer segment that had not been bleached initially was very rapid. Approximately 50% of the total increase in fluorescence achieved during the 50-min period after the second bleach was achieved within 1 min of the end of illumination. These results demonstrated that the initial local bleach primed the outer segment, so as to markedly facilitate the production of fluorescence subsequent to the second uniform bleach.

The data presented in Figs. 2 and 3 show that the fluorescence increase after bleaching occurred first in the most proximal portion of rod. The data in Fig. 4 imply that the presence of at least part of the inner segment (ellipsoid) is required for this wave-like increase to occur. The results illustrated in Fig. 5 show that this fluorescence is spatially restricted. A simple hypothesis, consistent with these results as well as those of Liebman (1969) and Hsu and Molday (1994), is that the substance responsible for the increase in fluorescence is all-trans retinol, after its reduction from all-trans retinal, and that the NADPH necessary for this reduction is supplied by synthetic reactions in the outer segment, as

well as other mechanisms involving mitochondria located in the ellipsoid region of the inner segment.

The experiments illustrated in Fig. 6 were designed to provide further tests of this hypothesis, by exposing bleached intact rods and isolated rod outer segments to solutions containing excess exogenous all-trans retinal and all-trans retinol. We reasoned that treatment of bleached cells with known concentrations of exogenous retinal or retinol could be used to test unequivocally the identity of the substrate of the reductase, and to test whether this reduction could be made to occur locally within intact outer segments. Fig. 6 A shows the time course of fluorescence changes within the outer segment of an intact rod that was first exhaustively bleached, after which it was superfused with a solution containing 1% ($\sim$150 µm) lipid-free BSA. Zero time in this plot corresponds to that at which the native bleach-induced fluorescence had reached its maximum. This is the time at which the cell was exposed to the 1% BSA to remove the bulk of the endogenous all-trans retinol produced subsequent to the bleach. The cell was then treated with a saline solution containing 1% BSA and 100 µM all-trans retinal to load the outer segment with exogenous retinal. It is apparent from the data presented in Fig. 6 A that exposure of the bleached cell to this retinal solution resulted in a large increase in outer segment fluorescence. The cell was returned to the 1% BSA solution once the fluorescence had reached a peak in order to test for the clearance of fluorescence by this lipophilic agent. These data demonstrate that treatment with exogenous all-trans retinal resulted in a substantial increase in the fluorescence signal that reached a final level that was $\sim$10-fold higher than that observed in normal cells after >99% pigment bleach. These data also demonstrate that the intact rod has a capacity to reduce retinal to retinol that is far greater than that necessary to deal with the amount of all-trans retinal normally produced by an exhaustive bleach of the native visual pigment. Furthermore, this retinol can be removed from the outer segment by BSA, as is expected to be the case with endogenous retinol.

Evidence that the fluorescence increase shown in Fig. 6 A is due to retinal reduction to retinol and that reduction requires the presence of the inner segment to occur is demonstrated in Fig. 6 (B–G). The graph in Fig. 6 B plots the spatial distribution of average fluorescence intensity along the longitudinal axis of uniformly bleached rod outer segments at different times after the exposure to all-trans retinal. The "0" position on the abscissa and dashed vertical line indicate the junction between the inner segment and the outer segment; the region at the base of the outer segment is plotted immediately to the right of the dashed line. The traces, from bottom to top, illustrate longitudinal fluorescence profiles before, and at 15, 45, and 60 min

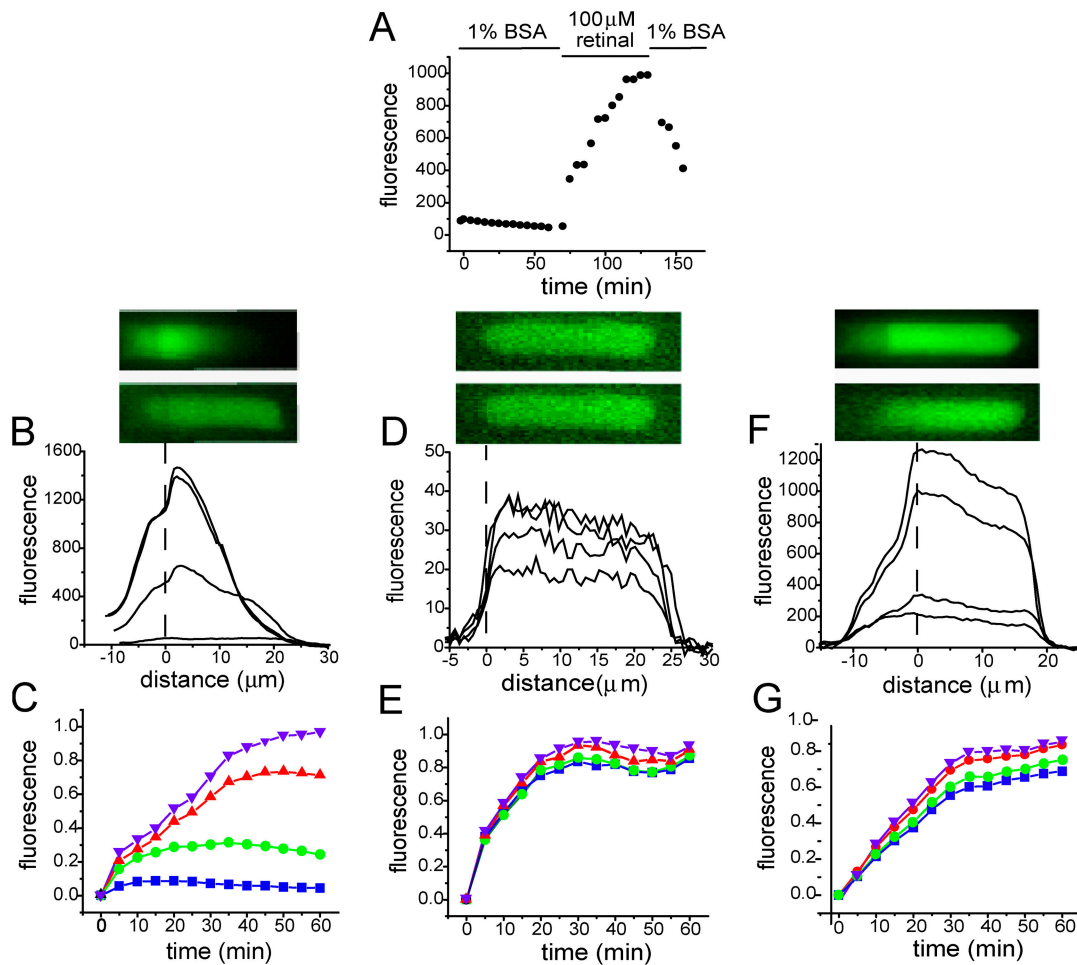436   *Retinol Fluorescence in Rods*

FIGURE 6. Response of bleached intact rod and isolated rod outer segments to exogenous all-trans retinal and all-trans retinol. (A) Fluorescence changes in a rod outer segment plotted versus time when cell was first bleached, then treated with a Ringer solution containing 1% BSA to remove endogenous all-trans retinol, then treated with BSA-Ringer solution containing 100 μM all-trans retinal to test the reducing capacity of the cell, and finally again treated with 1% Ringer-BSA solution to clear the fluorescence resulting from exogenous retinal treatment. Time = 0 corresponds to the time when, 60 min after the bleach, the endogenous outer segment fluorescence was at a maximal level. (B) Plot of longitudinal profiles of fluorescence intensity at different times before and after challenge with all-trans retinal. Profiles were taken (from bottom to top) at 0, 15, 45, and 60 min. The images above plot were taken before (bottom) and 60 min after treatment with all-trans retinal (top). Distance = 0 on the abscissa is the inner/outer segment border. (C) Time course of changes in fluorescence in four regions of the bleached outer segments of intact cells during challenge with all-trans retinal: proximal (▼), mid-proximal (▲), mid-distal (●), distal tip (■), $n = 5$. Symbols are colored for clarity. (D) Longitudinal profiles of fluorescence in bleached isolated outer segments treated with retinal at different times. Experimental parameters are as in A. Traces indicate profiles taken (from bottom to top) at 0, 5, 30, and 60 min. (E) Average time courses of fluorescence changes in four regions of isolated rod outer segment are not significantly different from one another; $n = 6$. The average fluorescence data in F and G were measured using the same protocol as in B and C, except that intact rods were treated with all-trans retinol rather than all-trans retinal; $n = 5$. Colored lines and symbols in E and G have the same significance as in C.

after exposure to the retinoid. Two fluorescence images of this cell, with the inner/outer segment junction positioned on the dashed line, are shown as two insets above this figure. These were taken 1 min before (bottom) and 60 min after (top) addition of the retinal-containing solution. Examination of these images together with the graph shows that after treatment with exogenous all-trans retinal, fluorescence was highly restricted to the region of the outer segment closest to the boundary between the inner and outer segment,

and that it diminished substantially in the more distal regions of the outer segment. Average results from four regions within the outer segments of five intact rods are shown in Fig. 6 C. The symbols used are the same as in Figs. 2 and 3, but have been colored for clarity. The bottom plot in this figure shows the time course of the fluorescence in the distal tip of the outer segment; the top plot is of the region of the outer segment closest to the inner/outer segment junction. Together, these plots emphasize that a >20-fold difference in fluores-

cence intensity developed between the proximal region of the outer segment and the distal tip of the cell located 20 μm away.

Fluorescence profiles were measured on rod outer segments that were isolated from the ellipsoid/inner segment and treated in the same way as in Fig. 6 (B and C). These results are illustrated in Fig. 6 (D and E). Examination of the longitudinal fluorescence profiles in these isolated outer segments (Fig. 6 D, graph and two fluorescence images), as well as the regional temporal increases in fluorescence (Fig. 6 E) after exposure to retinal, showed that a substantial increase in fluorescence is observed in these truncated outer segments treated in this way, but that no significant gradient could be observed along the long axis of the isolated outer segment after retinal treatment. These experiments illustrate that the inner segment/ellipsoid region of the cell is important for the reduction of exogenous retinal by intact outer segments.

The plots in Fig. 6 (F and G) illustrate the results of experiments similar to those shown in Fig. 6 (B and C), except that bleached intact rods were treated with all-trans retinol rather than all-trans retinal. As expected, retinol treatment resulted in a substantial increase in the overall fluorescence of the outer segment of the rod, as occurred after treatment with all-trans retinal. However, the spatial gradient of fluorescence observed after treatment with retinol was much less pronounced (Fig. 6, compare B and C with F and G). It is apparent that both retinal and retinol are able to partition into the outer segment membranes, but only all-trans retinal treatment results in a large gradient of fluorescence in the outer segment. Furthermore, the production of this gradient occurs only in intact cells that contain a functional inner segment. Isolated rod outer segments have a much diminished capacity to generate fluorescence after challenge with all-trans retinal, and they are unable to produce a gradient of fluorescence along their longitudinal axis.

All of the data presented here are consistent with the notion that the outer segment fluorescence we observed after bleaching is due to a persistent accumulation of all-trans retinol. If this is so, how then is all-trans retinol cleared from the rod outer segments and subsequently translocated to the retinal pigment epithelium? The retinoid transport/buffer proteins IRBP and RBP (serum retinol binding protein), as well as serum albumin have been identified in the interphotoreceptor matrix (Jones et al., 1989; for review see Pepperberg et al., 1993). The plots in Fig. 7 (A and B) are presented to show the effects that treatment with IRBP or BSA has on bleach-induced fluorescence in rod outer segments at concentrations extending over the physiological range. In these measurements, intact rods were first exhaustively bleached and tested periodically in darkness
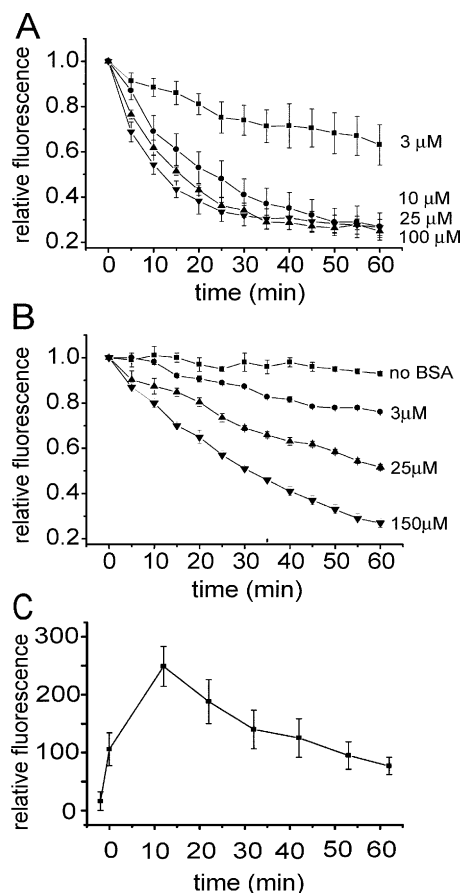

FIGURE 7. Time course of clearance of all-trans retinol from outer segments of bleached intact rods during treatment with IRBP and BSA. In A and B, rods were first bleached, and the increase in outer segment fluorescence was followed for 1 h until it had achieved its stable maximum value. (A) Cells were then treated (T = 0) with 3 μM (■), 10 μM (●), 25 μM (▲), or 100 μM (▼) IRBP, and the change in fluorescence was followed in subsequent darkness for 60 min. (B) Cells bleached and left in darkness as in A, and then treated as in A with BSA-free (■), 3 μM (●), 25 μM (▲), and 150 μM (▼) BSA solution. The change in fluorescence was followed in subsequent darkness for 60 min. All data in A and B were plotted as the mean (±SEM, $n = 3$). (C) Plot of average change (±SEM, $n = 5$) before and after total bleach in intact rods maintained in 100 μM IRBP solution. See text for additional details.

over the subsequent 60 min after bleaching to determine that the endogenous retinol fluorescence had stabilized at maximum levels. Cells were then challenged with different concentrations of IRBP (Fig. 7 A) or BSA (Fig. 7 B) to determine the rate of decline of fluorescence over the next 60 min. The rate of decline of fluorescence when both IRBP and BSA were withheld from the medium is shown by the filled squares in Fig. 7 B. It is apparent from examination of these data that both of these lipophilic agents are useful in effecting a time-dependent decrease in fluorescence; however, on a molar basis, IRBP is the more effective of the two substances.
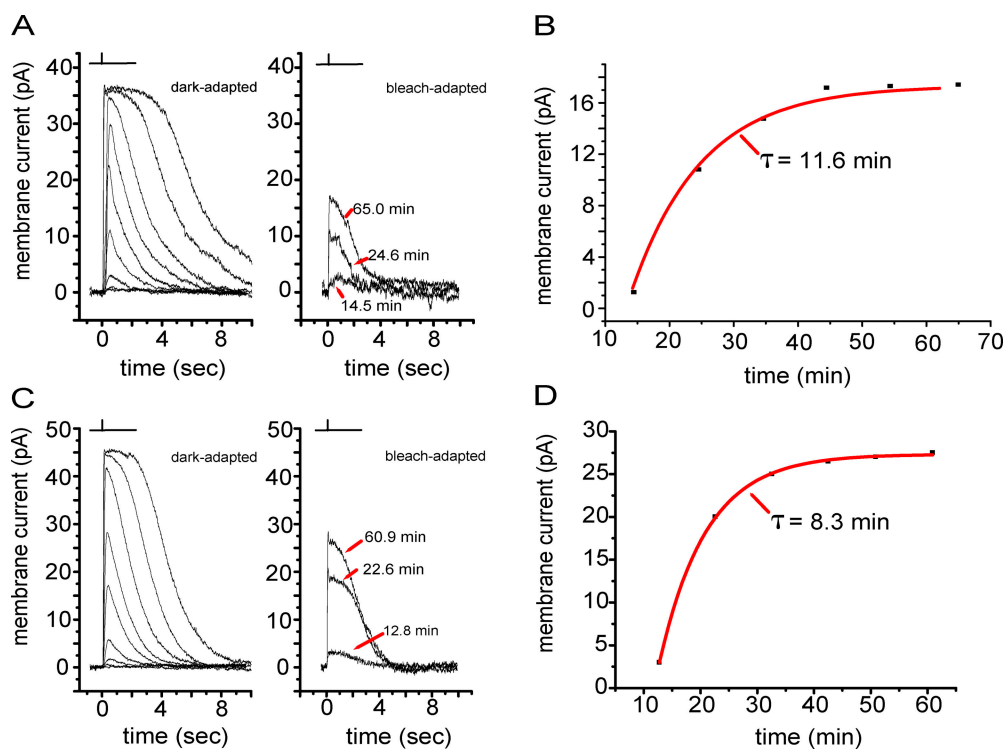
FIGURE 8. Flash responses measured in normal and IRBP-containing solution. (A) Left, family of responses to different intensity flashes measured in a rod prior to exposure to a bleaching light calculated to have bleached >99% of the pigment. Right, three saturating responses measured after different times in subsequent darkness. (B) Time course of increase in the saturating flash response amplitude was measured as in A. Smooth curve fitted as a single exponential function (τ = 11.6 min). (C) Responses measured as in A, except cell bathed in 100 μM IRBP solution. (D) Data from C plotted as in B. Smooth curve fitted as a single exponential function (τ = 8.3 min).

Moreover, in striking contrast to albumin, IRBP exhibits an apparent saturation at 10 μM. This result would suggest that there are specific binding sites on the photoreceptor cells for IRBP that facilitate clearance.

Fig. 7 C illustrates the averages of data collected from five experiments in which fluorescence was measured from the outer segments of intact rod cells that were bleached in the presence of 100 μM IRBP. This represents more closely the medium that normally bathes the receptors. Here, it can be seen that the maximum amplitude of the fluorescence signal achieved after the bleach is only ∼25% of that observed when IRBP is not present (see Fig. 2 B), and peaks earlier. Furthermore, the fluorescence change is transient. We assume that this represents more closely the time course of the change in the concentration of all-trans retinol in rod outer segments in the intact retina.

Fig. 8 illustrates data from electrophysiological experiments to compare the time course of the recovery of responsiveness (dark current) of intact rods after bleaching in the presence and absence of IRBP. These experiments were designed to determine if the clearance of retinoid in darkness from bleached rods can accelerate the recovery of flash response amplitude. The inner segment of the cell was drawn into a glass recording pipette, as illustrated in Fig. 1 A (left). Since the cell was isolated from the RPE, no pigment regeneration was possible (Cornwall et al., 1983). Fig. 8 A (left) shows a family of electrical responses to test flashes of varying intensity, elicited from a dark-adapted intact

rod bathed in medium that was free of IRBP or BSA. The cell was then exhaustively bleached. For about the first 10 min after bleaching, the cell was observed to be unresponsive to flashes of any intensity, after which flash response amplitude slowly recovered. The responses in Fig. 8 A (right) were elicited by bright supersaturating flashes after this unresponsive period. These latter flashes were of a light intensity designed to measure the maximum level of the dark current as the cell recovered. Fig. 8 B shows the recovery time course of the maximum amplitude of the dark current, as measured from the maximum amplitude of the responses shown in Fig. 8 A after the delay period during which the cell was unresponsive. These data are fitted to a single exponential curve with a time constant of 11.6 min. The average time constant of data derived from nine such cells was 14.9 ± 1.3 min (SEM). Fig. 8 C shows data from another experiment similar to that in Fig. 8 A, except that the cell was superfused with the same medium as in Fig. 8 A to which 100 μM IRBP was added. The time course of recovery of the light-suppressible dark current in this cell is shown in Fig. 8 D. Here, the time constant of the curve fitted to the data was 8.3 min. The average time constant of recovery of six bleach-adapted cells treated in this way was 8.6 ± 0.8 min (SEM). However, the average fraction of total current recovery in rods bleached in the presence or absence of IRBP was not significantly different.

Fig. 9 illustrates a bar graph that compares averages from experiments performed as in Fig. 8. Here, the de-
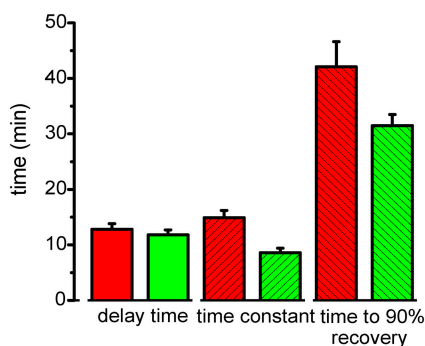
439   TSINA ET AL.

FIGURE 9. Bar graphs showing time delay to start of recovery of saturated flash responses, time constant for recovery of these responses after initial delay, and total time for recovery of response amplitude to 90% of post-bleach steady-state value after bright light. Measurements made in isolated intact rods. Bar amplitude shows mean ± SEM in normal solution (left, red) and 100 μM IRBP-containing solution (right, green). Tabulated mean values (±SEM) were as follows: delay in Ringer, 12.8 ± 1.0 min; delay in 100 μM IRBP, 11.8 ± 0.9; time constant (τ) in Ringer, 14.3 ± 0.9 min; time constant (τ) in 100 μM IRBP, 8.6 ± 0.8 min; recovery time (90%) in Ringer, 42.1 ± 4.5 min; recovery time (90%) in 100 μM IRBP, 31.5 ± 2.0 min.

lay time before measurable current recovery, the recovery time constant (τ), and total time for the dark current to recover to 90% of its post-bleach steady-state value are compared. It can be seen from examination of this graph that the delay times in these two conditions were indistinguishable, whereas both the time constant and the time for 90% current recovery were significantly shorter in IRBP-containing medium.

DISCUSSION

The experiments described here were designed to make direct microfluorometric measurements of the spatial distribution and kinetics of the reduction of all-trans retinal to all-trans retinol after exposure to bright bleaching light in intact salamander red rods, as well as to measure the clearance of all-trans retinol from these cells in subsequent darkness. In addition, we sought to determine if the reduction of retinal to retinol contributes to quenching of the sustained activation of the transduction cascade that follows light activation in these rods, and thereby facilitates recovery of responsiveness. There are three principal results of our studies. First, after bleaching, an intrinsic green fluorescence attributable to the reduction of all-trans retinal to all-trans retinol appears in the outer segments. This fluorescence increases as a wave, starting at the base of the outer segment and proceeds toward the distal tip. Second, in the absence of retinoid-binding proteins in the extracellular medium, retinol fluorescence is persistent, declining very slowly in darkness after having reached its peak. Third, the clearance of retinoids from bleached rod outer segments by IRBP modestly acceler-

ates the recovery of the light-suppressible current in darkness after the bleach.

Mechanisms of Reduction of Retinal to Retinol: Sources of NADPH

A number of biochemical mechanisms have been identified by which the NADPH economy of rod photoreceptors may be regulated. One synthetic mechanism for the production of NADPH is by glycolysis and the hexose monophosphate pathways that operate within the outer segment (Futterman, 1963; McConnell et al., 1969; Futterman et al., 1970; Schnetkamp and Daemen, 1981; Hsu and Molday, 1991, 1994). A second mechanism is the phosphocreatine shuttle pathway, which is thought to transport high-energy phosphate groups in the form of creatine phosphate from the inner segment to the outer segment (Hsu and Molday, 1994). Finally, NADPH could be synthesized in the cytoplasm by NADP$^+$-dependent dehydrogenases that utilize substrates provided from the mitochondria in the ellipsoid region. Such mechanisms are well known to operate in other cell systems, but have not been specifically identified in rod cells.

These biochemical mechanisms provide a basis for understanding the wave-like behavior of retinol production we have observed. We propose that the wave-like gradient of retinal reduction to retinol most likely results from a gradient of NADPH along the long axis of the outer segment, since there is no axial gradient of visual pigment concentration in these cells as determined microspectrophotometrically (Williams, 1984), and the bleaching intensity in our experiments was uniform throughout the cell. We propose that under our experimental conditions, NADPH is available from at least two different pools for the reduction of retinal to retinol. The rapid initial reduction of retinal that occurs within the first 2 min of the end of the bleach (see Fig. 3 B and Fig. 4 A, respectively) uses a pool of NADPH that is either resident in the outer segment in darkness before the bleach, or is provided by an as yet unidentified rapid synthetic mechanism. After this initial period, the cell must rely on NADPH that is newly synthesized by slower processes. We propose that one of these processes involves the glycolytic and hexose monophosphate pathways reviewed above. Under the extreme conditions of bleaching that prevail in our studies, a gradient of NADPH might be expected to be secondary to a gradient of ATP concentration that results from the diffusion of creatine phosphate from regions within the ellipsoid. Evidence for such a gradient of ATP along the long axis of the outer segment has been provided in studies of frog rods in intact retinas incubated with radiolabeled orthophosphate (Paulsen and Schurhoff, 1979; Paulsen and Rudolphi, 1980). Thus, a gradient of ATP along the long axis of the

outer segment could limit the phosphorylation of glucose by hexokinase at the tip of the outer segment relative to the base, and lead to a gradient-wise production of retinol when the outer segment is exposed to a high-level bleach.

Clearance of Retinol from Bleached Rods

When no lipophilic agent such as IRBP or BSA is included in the superfusate (such substances are normally present in the interphotoreceptor matrix), fluorescence of intact rods is persistent, spontaneously declining by <5% in darkness over a period of 1 h, after it reaches its peak. These data argue that clearance mechanisms external to the cell in the extracellular matrix of the retina likely operate to facilitate removal of all-trans retinol from red rods after bleaching. The data in Fig. 7 suggest that one way in which this may occur in vivo is via binding to IRBP, serum albumin, or other lipophilic substances that may exist in the extracellular matrix. However, it is likely that other mechanisms are also involved, since the rate of clearance of retinol that we measure is slower than would be expected under normal physiological conditions.

The apparent saturation that we have observed in the clearance of all-trans retinol from bleached salamander red rods by IRBP at ~10 μM suggests the operation of specific binding sites for retinol on IRBP and for IRBP on the outer segment membrane. Support for the existence of specific retinoid binding sites comes from recent work demonstrating that there are three retinoid binding sites on IRBP. One of these has a broad ligand specificity and binds either all-trans retinol or 11-cis retinal. One of the two additional sites appears to be selective for all-trans retinol and the other for 11-cis retinal (Shaw and Noy, 2001). Evidence for binding sites for IRBP on photoreceptors has been found in cell biological studies of isolated mouse photoreceptor neurons in culture (Politi et al., 1989). These sites were shown to be concentrated primarily on the plasma membrane in the presumptive photoreceptor inner segment area. It was suggested that these binding sites could be involved in retinoid movement into and/or out of the cell. Our data shown in Figs. 6, 7, and 8 lend strong support to these ideas.

Physiological Correlates of Retinal to Retinol Reduction to Photoreceptor Sensitivity

The electrophysiological studies illustrated in Fig. 8 were performed on cells that had been isolated from the RPE, and were performed in the presence and absence of retinoid-binding proteins. This method has the significant advantage that the effects of pigment bleaching and retinoid transport can be examined separately, in the absence of pigment regeneration, as well

as in the presence or absence of retinoid-binding proteins. Under these special conditions, we observed that after substantial bleaching, there was a significant delay period during which the rod's response was completely refractory, followed by a period during which the response recovered as a simple exponential process (Fig. 8). The average time constant for response recovery measured under these conditions (14.9 min; Fig. 8) is very close to that measured for the increase in fluorescence after bleaching (12.8 min; Fig. 3), but it is difficult to determine how the two phenomena are related. Our measurement of these two processes was not made at the same point in time relative to that of the bleach; the increase in the fluorescence signal started within a minute of bleaching (Figs. 2 and 3), whereas the recovery of the dark current was delayed on average by >11 min (Fig. 7, B and D). However, if the fitting of the red line shown in Fig. 3 B is restricted to only those points after 10 min, the time constant remains essentially the same as is shown. An intriguing possibility is that at these bleaching levels, current recovery may be rate limited by retinal-to-retinol reduction, but only after recovery from a saturated process that has resulted in total suppression of the dark current for a considerable time after bleaching. It is not possible to determine from our data what other processes may be involved in dark adaptation, but recent experiments on bleached mouse retina have demonstrated that under normal physiological conditions, the recovery of sensitivity is more likely to be due to multiple phosphorylation of the bleached photopigment (Kennedy et al., 2001).

Our data presented in Figs. 8 and 9 demonstrate that the presence of IRBP in the medium bathing rods is effective in a modest acceleration in the recovery of receptor dark current that leads to recovery of flash response amplitude after bleaching light. On average, the time for recovery of response amplitude (90% of steady-state) was shortened from 42 to 32 min. These data, together with that demonstrating that IRBP facilitates the removal of retinol from bleached rods (Fig. 7), suggest that, under the conditions of our experiments, IRBP either may accelerate the clearance of retinol from the outer segment thereby facilitating the reduction of retinal to retinol by mass action, or it may promote the clearance of retinal directly. In either case, facilitated clearance of retinal under our experimental conditions appears to shorten the total time for recovery of the dark current after the bleach. This conclusion is consistent with a large body of biochemical as well as physiological evidence that has demonstrated that all-trans retinal can combine in vitro with opsin to form complexes similar to Meta II that have significant G-protein activity. Additionally, Meta II and Meta II–like bleaching photoproducts have been implicated in numerous studies of rods (Leibrock et al., 1994, 1998;

Leibrock and Lamb, 1997) to limit recovery of visual sensitivity after bright light. Therefore, we propose that IRBP and other related proteins that are normally present in the interphotoreceptor matrix may aid in the clearance of retinoids from rod photoreceptors and thereby accelerate the recovery of the receptor current.

R E F E R E N C E S

Adler, A.J., and R.B. Edwards. 2000. Human interphotoreceptor matrix contains serum albumin and retinol-binding protein. *Exp. Eye Res.* 70:227–234.

Adler, A.J., C.D. Evans, and W.F. Stafford III. 1985. Molecular properties of bovine interphotoreceptor retinol-binding protein. *J. Biol. Chem.* 260:4850–4855.

Baylor, D.A., T.D. Lamb, and K.W. Yau. 1979. The membrane current of single rod outer segments. *J. Physiol.* 288:589–611.

Bernstein, P.S., and R.R. Rando. 1986. In vivo isomerization of all-trans- to 11-cis-retinoids in the eye occurs at the alcohol oxidation state. *Biochemistry.* 25:6473–6478.

Cornwall, M.C., A. Fein, and E.F. MacNichol Jr. 1983. Spatial localization of bleaching adaptation in isolated vertebrate rod photoreceptors. *Proc. Natl. Acad. Sci. USA.* 80:2785–2788.

Cornwall, M.C., A. Fein, and E.F. MacNichol Jr. 1990. Cellular mechanisms that underlie bleaching and background adaptation. *J. Gen. Physiol.* 96:345–372.

Cornwall, M.C., G.J. Jones, V.J. Kefalov, G.L. Fain, and H.R. Matthews. 2000. Electrophysiological methods for measurement of activation of phototransduction by bleached visual pigment in salamander photoreceptors. *Methods Enzymol.* 316:224–252.

Cornwall, M.C., E.F. MacNichol Jr., and A. Fein. 1984. Absorptance and spectral sensitivity measurements of rod photoreceptors of the tiger salamander, *Ambystoma tigrinum. Vision Res.* 24:1651–1659.

Corson, D.W., V.J. Kefalov, M.C. Cornwall, and R.K. Crouch. 2000. Effect of 11-cis 13-demethylretinal on phototransduction in bleach-adapted rod and cone photoreceptors. *J. Gen. Physiol.* 116:283–297.

Dartnall, H.J.A. 1972. Photosensitivity. *In* Handbook of Sensory Physiology. Vol. VII/1. H.J.A. Dartnall, editor. Springer Verlag, Berlin. 122–145.

Futterman, S. 1963. Metabolism of the retina. *J. Biol. Chem.* 238:1145–1150.

Futterman, S., A. Hendrickson, P.E. Bishop, M.H. Rollins, and E. Vacano. 1970. Metabolism of glucose and reduction of retinaldehyde in retinal photoreceptors. *J. Neurochem.* 17:149–156.

Govardovskii, V.I., N. Fyhrquist, T. Reuter, D.G. Kuzmin, and K. Donner. 2000. In search of the visual pigment template. *Vis. Neurosci.* 17:509–528.

Hsu, S.C., and R.S. Molday. 1991. Glycolytic enzymes and a GLUT-1 glucose transporter in the outer segments of rod and cone photoreceptor cells. *J. Biol. Chem.* 266:21745–21752.

Hsu, S.C., and R.S. Molday. 1994. Glucose metabolism in photoreceptor outer segments. Its role in phototransduction and in NADPH-requiring reactions. *J. Biol. Chem.* 269:17954–17959.

Jones, G.J., R.K. Crouch, B. Wiggert, M.C. Cornwall, and G.J. Chader. 1989. Retinoid requirements for recovery of sensitivity after visual-pigment bleaching in isolated photoreceptors. *Proc. Natl. Acad. Sci. USA.* 86:9606–9610.

Kaplan, M.W. 1985. Distribution and axial diffusion of retinol in bleached rod outer segments of frogs (*Rana pipiens*). *Exp. Eye Res.* 40:721–729.

Kennedy, M.J., K.A. Lee, G.A. Niemi, K.B. Craven, G.G. Garwin, J.C. Saari, and J.B. Hurley. 2001. Multiple phosphorylation of rhodopsin and the in vivo chemistry underlying rod photoreceptor dark adaptation. *Neuron.* 31:87–101.

Kuhne, W. 1879. Chemische vorgange in der netzhaut. Vol. 3. L. Hermann, editor. F.C.W. Vogel, Leipzig. Translated by R. Hubbard, and G. Wald. 1977. Chemical processes in the retina. *Vision Res.* 17:1273–1316.

Lamb, T.D., P.A. McNaughton, and K.W. Yau. 1981. Spatial spread of activation and background desensitization in toad rod outer segments. *J. Physiol.* 319:463–496.

Leibrock, C.S., and T.D. Lamb. 1997. Effect of hydroxylamine on photon-like events during dark adaptation in toad rod photoreceptors. *J. Physiol.* 501:97–109.

Leibrock, C.S., T. Reuter, and T.D. Lamb. 1994. Dark adaptation of toad rod photoreceptors following small bleaches. *Vision Res.* 34:2787–2800.

Leibrock, C.S., T. Reuter, and T.D. Lamb. 1998. Molecular basis of dark adaptation in rod photoreceptors. *Eye.* 12:511–520.

Liebman, P.A. 1969. Microspectrophotometry of retinal cells. *Ann. NY Acad. Sci.* 157:250–264.

Liebman, P.A. 1973. Microspectrophotometry of visual receptors. *In* Biochemistry and Physiology of Visual Pigments. H. Langer, editor. Springer-Verlag, Berlin. 299–305.

Liebman, P.A., and G. Entine. 1974. Lateral diffusion of visual pigment in photoreceptor disk membranes. *Science.* 185:457–459.

Lion, F., J.P. Rotmans, F.J. Daemen, and S.L. Bonting. 1975. Biochemical aspects of the visual process. XXVII. Stereospecificity of ocular retinol dehydrogenases and the visual cycle. *Biochim. Biophys. Acta.* 384:283–292.

McBee, J.K., V. Kuksa, R. Alvarez, A.R. de Lera, O. Prezhdo, F. Haeseleer, I. Sokal, and K. Palczewski. 2000. Isomerization of all-trans-retinol to cis-retinols in bovine retinal pigment epithelial cells: dependence on the specificity of retinoid-binding proteins. *Biochemistry.* 39:11370–11380.

McConnell, D.G., G.W. Ozga, and D.A. Solze. 1969. Evidence for glycolysis in bovine retinal microsomes and photoreceptor outer segments. *Biochim. Biophys. Acta.* 184:11–28.

Okajima, T.I., D.R. Pepperberg, H. Ripps, B. Wiggert, and G.J. Chader. 1990. Interphotoreceptor retinoid-binding protein promotes rhodopsin regeneration in toad photoreceptors. *Proc. Natl. Acad. Sci. USA.* 87:6907–6911.

Palczewski, K., S. Jager, J. Buczylko, R.K. Crouch, D.L. Bredberg, K.P. Hofmann, M.A. Asson-Batres, and J.C. Saari. 1994. Rod outer segment retinol dehydrogenase: substrate specificity and role in phototransduction. *Biochemistry.* 33:13741–13750.

Paulsen, R., and P. Rudolphi. 1980. Rhodopsin phosphorylation in the frog retina: analysis by autoradiography. *Neurochem.* 1:2870289.

Paulsen, R., and K. Schurhoff. 1979. The localization of phosphorylated rhodopsin in the frog rod outer segment. *Eur. J. Cell Biol.* 19:35–39.

Pepperberg, D.R., T.L. Okajima, B. Wiggert, H. Ripps, R.K. Crouch, and G.J. Chader. 1993. Interphotoreceptor retinoid-binding pro-

tein (IRBP). Molecular biology and physiological role in the visual cycle of rhodopsin. *Mol. Neurobiol.* 7:61–85.

Politi, L.E., L. Lee, B. Wiggert, G. Chader, and R. Adler. 1989. Synthesis and secretion of interphotoreceptor retinoid-binding protein (IRBP) by isolated normal and rd mouse retinal photoreceptor neurons in culture. *J. Cell. Physiol.* 141:682–690.

Pugh, E.N., and T.D. Lamb. 2000. Phototransduction in Vertebrate Rods and Cones: Molecular Mechanisms of Amplification, Recovery, and Light Adaptation. Vol. 3. Elsevier Science Publishing Co. Inc., New York. 183–255.

Rattner, A., P.M. Smallwood, and J. Nathans. 2000. Identification and characterization of all-trans-retinol dehydrogenase from photoreceptor outer segments, the visual cycle enzyme that reduces all-trans-retinal to all-trans-retinol. *J. Biol. Chem.* 275: 11034–11043.

Redmond, T.M., B. Wiggert, F.A. Robey, N.Y. Nguyen, M.S. Lewis, L. Lee, and G.J. Chader. 1985. Isolation and characterization of monkey interphotoreceptor retinoid-binding protein, a unique extracellular matrix component of the retina. *Biochemistry.* 24: 787–793.

Saari, J.C., D.L. Bredberg, and D.F. Farrell. 1993. Retinol esterification in bovine retinal pigment epithelium: reversibility of lecithin:retinol acyltransferase. *Biochem. J.* 291:697–700.

Schnetkamp, P.P., and F.J. Daemen. 1981. Transfer of high-energy phosphate in bovine rod outer segments. A nucleotide buffer system. *Biochim. Biophys. Acta.* 672:307–312.

Shaw, N.S., and N. Noy. 2001. Interphotoreceptor retinoid-binding protein contains three retinoid binding sites. *Exp. Eye Res.* 72: 183–190.

Tsin, A.T., H.A. Pedrozo-Fernandez, J.M. Gallas, and J.P. Chambers. 1988. The fluorescence quantum yield of vitamin A2. *Life Sci.* 43: 1379–1384.

Wald, G., and R. Hubbard. 1949. The reduction of retinene1 to vitamin A1 in vitro. *J. Gen. Physiol.* 32:367–389.

Williams, T.P. 1984. Some properties of old and new rhodopsin in single Bufo rods. *J. Gen. Physiol.* 83:841–852.